Proc. of 1st KSV Conference
KAIST, Daejeon, KOREA, Nov. 8, 2002

레이저와 질소가스 상호충돌로부터 발생되는 플라스마 가시화

김종욱†* · 김창범* · 김광훈* · 이해준* · 석희용*

Visualization of Plasma Produced in a Laser Beam and Gas Jet Interaction

Jong-Uk Kim†* · Chang-Bum Kim* · Guang-Hoon Kim* · Hae-June Lee* · Hy-Yong Suk*

Abstract

In the current study, characteristics of the laser-induced plasma were investigated in a gas filled chamber or in a gas jet by using a relatively low intensity laser ($I \leq 5 \times 10^{12}$ W/cm^2). Temporal evolutions of the produced plasma were measured using the shadow visualization and the shock wave propagation as well as the electron density profiles in the plasma channel was measured using the Mach-Zehnder interferometry. Experimental results such as the structure of the produced plasma, shock propagation speed (V_s), electron density profiles (n_e), and the electron temperature (T_e) are discussed in this study. Since the diagnostic laser pulse occurs over short time intervals compared to the hydrodynamic time scales of expanding plasma or a gas jet, all the transient motion occurring during the measurement is assumed to be essentially frozen. Therefore, temporally well-resolved quantitative measurements were possible in this study.

Key Words : Laser-Induced Plasma (레이저유도 플라스마) Plasma Visualization(플라스마 가시화)

1. INTRODUCTION

Propagation of an intense laser pulse through fully ionized plasma has been an interesting topic in many fields. It includes laser-driven electron accelerators,[1] generation of high harmonics,[2] and soft x-ray laser development.[3] The plasma wave-guide has made possible one of the major goals in intense laser-matter interaction physics. Since relatively large volume of plasma can be obtained in a gas jet and the produced plasma is fairly stable during the laser pulse duration, pulsed gas jet has been employed for a useful target in the study of laser-plasma interaction.[4] In order to study optical guiding of an intense laser pulse through ionized plasma, investigation on the characteristic of the ionized plasma itself should be made in advance. Important to this application is detailed knowledge of shock dynamics including generation of the shock wave and its spatial- and temporal- evolution in the plasma, which leads the electron density profiles forming the wave-guide. In this paper, we report both the Mach-Zehnder and Shadowgraph measurements of the laser-induced plasma (LIP) produced by breakdown of neutral nitrogen gas (N_2) at the focal spot of the laser.

† Korea Electrotechnology Research Institute
Center for Advanced Accelerators
E-mail: jukim@keri.re.kr
* Korea Electrotechnology Research nstitute
Center for Advanced Accelerators

2. EXPERIMENTAL SET-UP

The present study reports shadowgraph as well as the Mach-Zehnder interferometer measurements of the laser-induced plasma, produced by N_2 gas breakdown, at the focal spot of a laser. Schematic of the experimental setup for the laser-induced plasma is shown in Fig. 1. Breakdown of N_2 gas was obtained by focusing (with a 150 mm focal length lens) a beam from a Q-switched Nd:YAG laser (Spectra Physics, Model Quanta-Ray Pro 290). The laser was operated at the second harmonic (λ = 532 nm) and 10 Hz repetition rate with 7 ns pulse duration of full width at half maximum (FWHM) and 6 mm beam diameter. The peak power of the laser pulse at 532 nm is approximately 0.13 GW and the beam size at the focal point is approximately 40 μm. Therefore, beam intensities at the focal point is approximately 5.7×10^{12} W/cm^2. The laser-induced plasma is located in one arm of the Mach-Zehnder interferometer, which is illuminated with an attenuated and expanded beam from a second harmonic of an Nd:YAG laser.

In order to probe the produced plasma, we split off small amount of the main (532 nm) beam (≈ 4%) and this

diagnostic beam travels a long delay leg and illuminates the plasma channel at a right angle to the propagation of the main pulse. The probe beam that traverses the plasma channel is interfered with a reference beam and produces interferograms in a commercially available Kodak DC 260 1536×1024 digital CCD camera. The interferograms yield information on the phase shift resulting from the passages of the light through the plasma and the phase shift is Abel inverted to yield radial profiles of the electron density. Shadowgrams of the shock wave are also obtained by blocking the interferometer reference beam. Specifically, a point light source with significantly attenuated laser energy is required to increase the quality of the image; therefore, a 25 μm pinhole was employed in the measurement. The energy measured from the point light source was approximately 200 μJ. Images were obtained by projection onto a screen S, amplified, and recorded with a digital CCD camera, whose resolution is 7.5 μm × 7.5 μm. In order to collect the probe beam an interference filter (cutoff wavelength, $\lambda_c \geq 532$ nm) was employed in front of the detector. Except for the mirrors for optical delay all optics was included in the vacuum chamber, which maintains the internal pressure to the order of 10^{-4} Torr. The laser-induced plasma experiments were performed by changing the partial pressure of N_2 gas in the vacuum chamber (or, changing the backfill pressure of the nozzle in the gas jet) and by varying the laser energy from 100 mJ to 900 mJ. From the shadowgraphs as well as interferograms the temporal evolution of the plasma channel, shock wave, hot plasma core, and the electron density profiles were obtained to interpret their thermodynamic characteristics, which are closely related to the formation of the plasma channeling in the plasma.

3. RESULTS AND DISCUSSIONS

Typical example of a shadowgraph and a Mach-Zehnder interferogram of the laser-induced plasma produced by laser and N_2 gas interaction with laser energy of 700 mJ ~ 900 mJ were obtained at different time delay after N_2-gas breakdown and the images are shown in Fig. 2 and 3, respectively. In order to calculate the electron density profile the obtained fringe shifts were Avel-inverted. The radial electron density profiles at a specified time delay of 9.7 ns for both the 30 and 50 bar backfill pressure were measured with the laser energy of 900 mJ. At the shock-bound region (i.e., $r \leq 200$ μm) the 50 bar backfill pressure showed the electron density nearly 5 times higher than that of the 30 bar. Similar characteristics were observed also in the gas filled chamber when experiments were performed by changing the gas chamber pressure at fixed laser energy or, in reverse order. These results are shown in Fig. 4. As seen in the figure, at fixed chamber pressure (i.e., 100 or 300 Torr) the electron densities measured with two different laser energies (i.e., 500 and 900 mJ) revealed no appreciable changes except slight increase the radius of the plasma channel. However, electron densities of ≈ 2.5×10^{18} cm^{-3} and ≈ 3.8×10^{18} cm^{-3} were measured at 100 and 300 Torr chamber pressure, respectively indicating that not the laser energy but the chamber gas pressure has the dominant role in determining the electron densities in the laser-induced plasma.

The expansion of the plasma channel in the gas-filled chamber was also observed for two chamber pressures (i.e., 100 and 300 Torr, respectively) and two laser energies (i.e., 250 and 450 mJ, respectively) and it is shown in Fig. 5. Zeldovich *et al.*, [5] developed a blast wave model, which describes the propagation of a shock wave caused by an instantaneous release of energy, E_{th}, through a background gas (density ρ_0). In this model, the propagation of the shock front follows the distance-time relation $R_s = \xi_0(E_{th}/\rho_0)^{1/5}t^{2/5}$, where ξ_0 is a constant. It strictly applies to an instantaneous energy release at a point. The position of the shock are least squares fitted to the expression, $R_s = \alpha t^{\beta}$, where α is a function of the pressure and laser energy. In our measurements, the fits yield $\beta \approx 0.40$ through 0.42 with maximum standard deviation of 0.01. This result is in excellent agreement with the point blast wave model $R_s \approx t^{2/5}$. Results showed that the shock front expands faster and further as the laser energy or the chamber gas pressure increases. Also, the shock wave separated from the hot plasma at early in time ($t \leq 1$ ns) and expanded faster and further after that. The decoupling of the shock wave from the hot plasma can be observed elsewhere, [6] and the collapse of the plasma is attributed to the rapid cooling with thermal diffusion to the outer layer of ionizing gas. Regardless of the parameters used in the measurements, a rapid decrease in shock expansion rate was found in the first 5 ns. The highest shock speed was found in the case of 300 Torr, 450 mJ with an approximate value of ≈ 4.1×10^6 cm/sec. It is interesting to note that the shock expansion rates for both the 300 torr 250 mJ and 100 torr 450 mJ cases are very much similar in time. At the maximum delay of 70 ns, all of the shock speed approaches to ≈ (2-4) × 10^5 cm/sec.

Assuming that the plasma pressure is much greater than the background pressure electron temperature (T_e) [7] can be estimated by the shock speed (V_s) expression; $V_s \approx [\gamma Z^* kT_e/M_i]^{1/2}$, where γ is the specific heat ratio (≈1), Z^* and M_i are ionization level and mass of the gas, respectively and k is the Boltzmann's constant. By using this expression, the electron temperature at $t \approx 1$ ns (i.e., at the highest shock speed of $V_s \approx 4.1 \times 10^6$ cm/sec for the 300 torr 450 mJ case) can be estimated to be $T_e \approx 2.4 \times 10^2$ eV. A rapid decrease in electron temperature could be found by $t \approx 7$ ns with $T_e \approx 24$ eV. Again, this is attributed to the rapid expansion of the shock wave by this time. At the maximum delay of $t \approx 70$ ns, when the shock speed approaches to $V_s \approx$ (2-4) × 10^5 cm/sec, the corresponding electron temperature was found to be less than 1.0 eV.

For the gas jet, the leading edge of the shock position was measured for three backfill pressures (30,

50, and 70 bar) at fixed laser energy of ≈900 mJ. Results showed that the shock position did not follow the least squares fit to the expression $R_s = \alpha t^{\beta}$. It rather followed a linear regression (i.e., $R_s \approx t$) at early in time (i.e., $1 \leq t \leq 10$ ns). It is interesting to note that the shock speed measured was inversely proportional to the applied backfill pressure with values of 12, 10.7, and 9.5×10^5 cm/sec for 30, 50, and 70 bar, respectively. The corresponding electron temperatures (T_e) were 1.7, 1.4, and 1.1×10^2 eV, respectively.

4. CONCLUSIONS

In conclusion, a relatively low intensity laser ($I \leq 5\times10^{12}$ W/cm^2) was used to investigate the laser-induced plasma in a gas filled chamber and in a gas jet. Optical imaging methods including the Mach-Zehnder interferometry and shadowgraphy were employed in the study. Experimental results showed that the shapes of the laser-induced plasma were very differed with gas pressure applied in the chamber and even more they were quite dependent on the laser energy applied. Temporal evolutions of the laser-induced plasma were also observed and the results showed that as time increased the produced plasma propagated backward direction (i.e., to the focusing lens) with decreasing the plasma width regardless of the gas pressures applied in the chamber. The shock wave separated from the hot plasma core early in time ($t \leq 1$ ns) and the shock expansion speed was increased faster and further with increasing the laser energy or the gas pressure in the chamber. Also, the possible wave-guiding mode was not observed in the gas filled chamber. On the other hand, electron density minimum on-axis (i.e., possible wave guiding mode) was observed in a gas jet with initial shock expansion speed of $\approx 1.0 \times 10^6$ cm/sec and corresponding electron temperature of $\approx 1.0 \times 10^2$ eV.

Further studies are required, however, to understand more carefully the features of the laser-induced plasma that are closely related to the applied gas pressure and the laser energy.

ACKNOWLEDGEMENT

Authors would like to thank for the financial support from the Korean Ministry of Science & Technology through the Creative Research Initiatives Program.

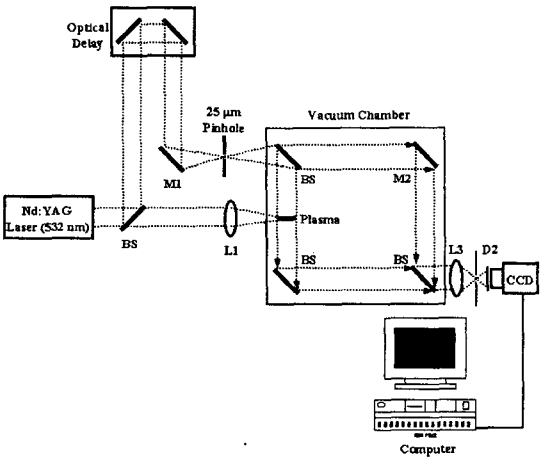

Figure 1. Schematic of the experimental setup of the laser-induced plasma (LIP).

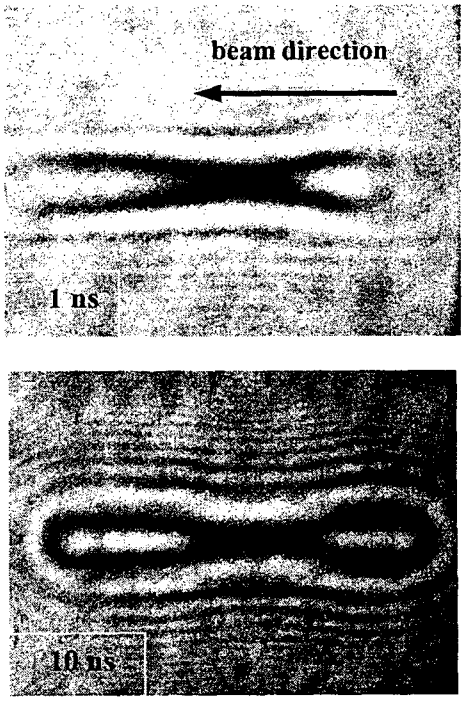

Figure 2. Typical example of a shadowgraph of the laser-induced plasma produced by laser and gas interaction with 240 Torr of N_2 gas at 700 mJ of laser energy.

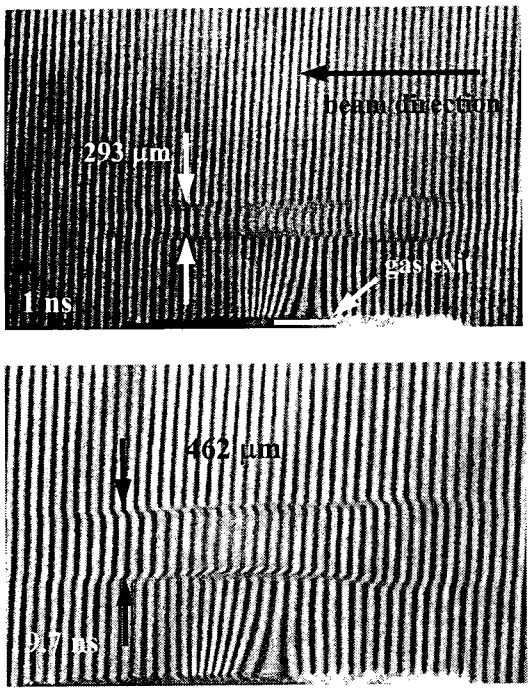

Figure 3. Typical interferograms of N_2 gas jet at two different time delays (1 and 9.7 ns) at 30 bar backfill pressure and 900 mJ of laser energy.

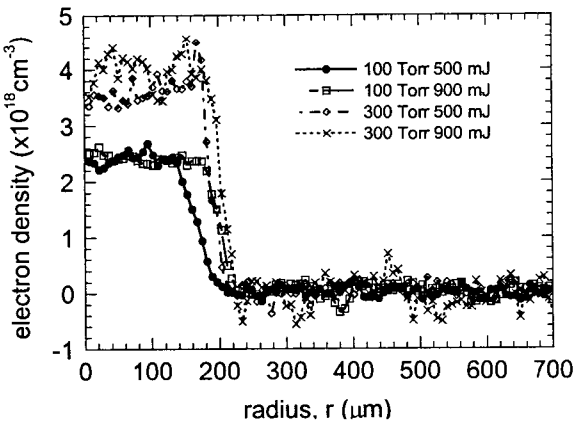

Figure 4. Electron density vs. radius of the gas filled chamber. Data were measured at 11 ns after plasma breakdown.

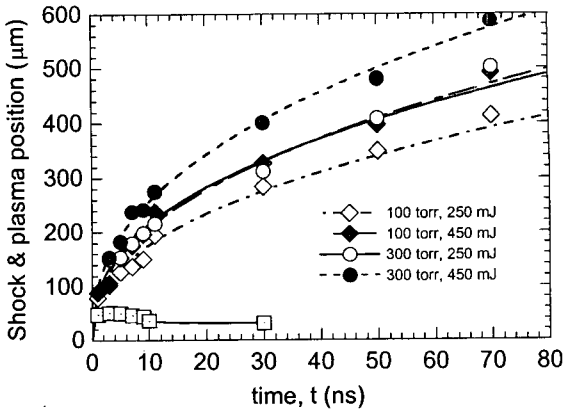

Figure 5. Shock (or Plasma) position *vs* time for different N_2 chamber pressure and laser energy. Least squares fits to $R_s = \alpha t^{\beta}$ are shown for each data.

REFERENCES

1. Tajima, T. and Dawson, J. M., 1979, "Laser electron accelerator," *Phys. Rev. Lett.* **43**, pp. 267-270.
2. Krause, J., Schafer, K. and Kulander, K., 1992, "High-order harmonic generation from atoms and ions in the high intensity regime," *Phys. Rev. Lett.* **68**, pp. 3535-3538.
3. Korobkin, D. V., Nam, C. H., Suckewer, S. and Goltsov, A., 1996, "Demonstration of soft X-ray lasing to ground state in Li III," *Phys. Rev. Lett.* **25**, pp. 5206-5209.
4. Wispelaere, E. De, Malka, V., Hüller, S., Amiranoff, F., Baton, S., Bonadio, R., Casanova, M., Dorchies, F., Haroutunian, R. and Modena, A., 1999, "Formation of plasma channels in the interaction of a nanosecond laser pulse at moderate intensities with helium gas jets," *Phys. Rev. E.* **59**, pp. 7110-7120.
5. Zeldovich, Y. A. and Raizer, Y. P., 1966, *Physics of Shock Waves and High-Temperature Hydrodynamic Phenomena* Academic Press, New York.
6. Kim, J. U., Clemens, N. T. and Varghese, P. L., 2002, "Characterization of a high density plasma produced by electrothermal capillary discharge," *Appl. Phys. Lett.* **80**, pp. 368-370.
7. Clark, T. R. and Milchberg, H. M., 1997, "Time- and space-resolved density evolution of the plasma waveguide," *Phys. Rev. Lett.* **78**, pp. 2373-2376.